Middle-East Journal of Scientific Research 26 (5): 543-554, 2018
ISSN 1990-9233

DOI: 10.5829/idosi.mejsr.2018.543.554

Analysis of the Effects of Concentration and Post Deposition Temperature on the Optical and Solid State Properties of Chemically Deposited $Zn_{1-x}O$ and $Co_{1-x}O$ Thin Films

[1,2]P.N. Kalu, [1]D.U. Onah, [2]P.E. Agbo, [1]C. Augustine,
[1]R.A. Chikwenze and [1]F.N.C. Anyaegbunam

[1]Department of Physics/Geology/Geophysics,
Alex Ekwueme Federal University Ndufu-Alike Ikwo, Ebonyi State, Nigeria
[2]Department of Industrial Physics, Ebonyi State University, Abakaliki, Nigeria

Abstract: $Zn_{1-x}O$ (x=0.7M, 0.5M and 0.3M) and $Co_{1-x}O$ (x=0.7M, 0.5M and 0.3M) thin films were deposited by chemical bath deposition method and the influence of concentration and annealing temperature on the optical and solid state properties were investigated. UV-VIS-NIR spectrophotometer was employed to characterize optical and solid state properties of the deposited films. The absorbance generally lie in the range $0.50 \leq A \leq 0.83$ for changes in the concentration of Zn^{2+} and $0.13 \leq A \leq 2.0$ for parametric variation of annealing temperature. With respect to variation in the concentration of Co^{2+}, the absorbance, A is within the range $0.13 \leq A \leq 2.13$ and in the range $0.80 \leq A \leq 2.10$ for variation of annealing temperature. It is found that the transmittance of $Zn_{1-x}O$ films decreased with concentration but increased with annealing temperature. $Zn_{1-x}O$ films transmittance transparency variesd from 25-88%, 20-68% and 15%-53% at 0.3M, 0.5M and 0.7M respectively. For $Co_{1-x}O$ films, it is noticed that the transmittance increasesd with precursor concentration from 2.5% to 60%, 2.5% to 80% and 2.5% to 85% for 03M, 0.5M and 0.7M respectively. Subjecting $Co_{1-x}O$ films to different temperatures, the transmittance varied from 10-68% for as-deposited, 2.5-77% for annealed at 100°C, 55-90% for annealed at 150°C and 10-74% for annealed at 200°C.The absorption coefficient, band gap energy, extinction coefficient, refractive index, real and imaginary dielectric constants were also affected by the growth parameters. In particular,parametric investigation involving changes in concentration of $Zn_{1-x}O$ films, E_g lie from 3.68-3.75eV whereas for variation of annealing temperature, $E_g$attenuates from 3.40 to 4.00 eV. The band gap of $Co_{1-x}O$ films at different concentration increased from 4.00eV to 4.05eV whereas the band gap values at different annealing temperature lie between 3.65-3.90. In view of the various wide band gap energy exhibited by the films, it can be concluded that they are promising window materials for solar cell fabrication as well as optoelectronic applications.

Key words: Band gap · Temperature · Thin film · Concentration · Optical

INTRODUCTION

In view of the urgent need to identify future sources of energy that will not only be affordable but also guarantees the safety of environment, it has become imperative to investigate the potentials of other inorganic materials that are non-toxic to the environment, abundant in nature and also posses easy fabrication techniques. Zinc oxide (ZnO) and Cobalt oxide (CoO) are among this category because the constituent elements are locally available and cost effective. More importantly, they have no direct contamination of the environment compared to those elements used in cadmium related devices such as in cadmium sulphide (CdS) and cadmium telluride (CdTe) solar cells. Zinc oxide (ZnO) is an important ll-Vl compound semiconductor with a wide band gap of about 3.37eV at room temperature [1]. ZnO has been used for the fabrication of light emitting diodes, photo detectors, piezoelectric cantilever, gas sensors, buffer layer in solar cell and in photonic crystals [2-7]. Cobalt oxide (Co_3O_4) is

Corresponding Author: P.N. Kalu, Department of Physics/Geology/Geophysics,
Alex Ekwueme Federal University Ndufu-Alike Ikwo, Ebonyi State, Nigeria.

an important p-type semiconductor with direct optical band gaps at 1.48eV and 2.19eV [8] and has been investigated extensively as promising materials in gas-sensing and solar energy absorption as well as an effective catalyst in environmental purification and chemical engineering [9, 10]. In addition, CoO thin film has been widely studied for its application as lithium ion battery electrodes, catalysts, ceramic pigments, field-emission materials and magnetic materials [11-14].

Diverse techniques have been employed to fabricate ZnO and CoO thin films including chemical vapour deposition [15, 16], spray pyrolysis [17, 18], sol-gel technique [19, 20], magnetic sputtering [21, 22], successive ionic layer adsorption and reaction technique (SILAR) [23, 24], chemical bath deposition [25, 26] among others. Chemical bath deposition method is one of the most widely used techniques in thin film deposition because it does not require sophisticated equipment and can easily be tailored to suit different device designs. The major objective of the present investigation is to access the potentials of a low cost and environmentally friendly inorganic materials (ZnO and CoO) for use in different optoelectronic and in electronic applications, including thin film solar cell devices. The variation of the optical and solid state parameters with parametric investigation involving concentration and post deposition temperature were analysed and discussed.

Experimental: $Zn_{1-x}O$ thin films were grown from a solution containing15mls of $ZnSO_4$(x = 0.7M, 0.5M and 0.3M), 5mls of ammonia and 15mls of water in that order at temperature of 70°C for 1 hour. The deposition of$Co_{1-x}O$ thin films was done from a chemical bath containing 15ml of $CoSO_4$(x = 0.7M, 0.5M and 0.3M), 5ml of NH_3 solution and 15ml of H_2O. The bath was maintained at a temperature of 70^0C for 1hour. Thermo scientific GENESYS 10S model UV-VIS spectrophotometer on the 300-1000 nm range of light at normal incidence to samples was used to obtain the absorbance data from which transmittance, absorption coefficient and band gap were calculated. The possible growth mechanism for the formation of $Zn_{1-x}O$ and $Co_{1-}O$ oxide thin films are shown below:

$$ZnSO_4 \rightarrow Zn^{2+} + SO_4{}^{2-}$$
$$NH_3.H_2O \rightarrow NH_4{}^{+} + OH^{-}$$
$$Zn^{2+} + OH^{-} \rightleftarrows Zn(OH)_2$$
$$Zn(OH)_2 \rightleftarrows ZnO + H_2O$$
$$C_o(SO_4)_2 \rightleftarrows Co^{2+} + SO_4{}^{2-}$$
$$Co^{2+} + 2(OH)^{-} \rightleftarrows Co(OH)_2$$
$$Co(OH)_2 \rightleftarrows CoO + H_2O$$

RESULTSAND DISCUSSION

The optical characterization of thin films involves measurement of optical properties such as absorbance, transmittance and reflectance from which absorption coefficient, band gap, refractive index, extinction coefficient, real and imaginary parts of dielectric constant were determined. Figures 1 and 2 show the plots of absorbance against wavelength for ZnO thin films at different concentration and post deposition temperature respectively while that of CoO films are shown in Figures 3 and 4 respectively.All the films are highly absorbent in UV.A glance over Figures 1 and 2, shows that growth parameters affected the films differently. The absorbance of ZnO films increased with concentration but decreased with post deposition temperature. The absorbance is generally higher for parametric variation involving post deposition temperature compared to that of concentration. The absorbance generally lie in the range $0.50 \leq A \leq 0.83$ for changes in the concentration of Zn^{2+} and $0.13 \leq A \leq 2.0$ at different annealing temperature. The absorbance spectra of $Co_{1-x}O$ grown under the same parametric conditions but treated to different post deposition temperature, reveals an increase in absorbance with increase in the concentration of Co^{2+} but shows no trend with respect to post deposition temperature. With respect to variation in the concentration of Co^{2+}, the absorbance, A is within the range $0.13 \leq A \leq 2.13$ and in the range $0.80 \leq A \leq 2.10$ for variation of annealing temperature. The plots of transmittance against wavelength of $Zn_{1-x}O$ thin films at different concentration and annealing temperatures are shown in Figures 5 and 6 respectively. Figures 7 and 8 are the plots of transmittance against wavelength of $Co_{1-x}O$ thin films at different annealing temperature and concentration respectively.

In all deposition parameters, transmittance increases of the films in UV-VIS-NIR is found to increase with wavelength. It turns out that the transmittance of $Zn_{1-x}O$ films decreased with concentration but increased with annealing temperature. $Zn_{1-x}O$ films transmittance transparency varied from 25-88%, 20-68% and 15%-53% at 0.3M, 0.5M and 0.7M respectively. The decrease in transmittance with concentration is in consonance with the report in the following reference in the literature [27-29].

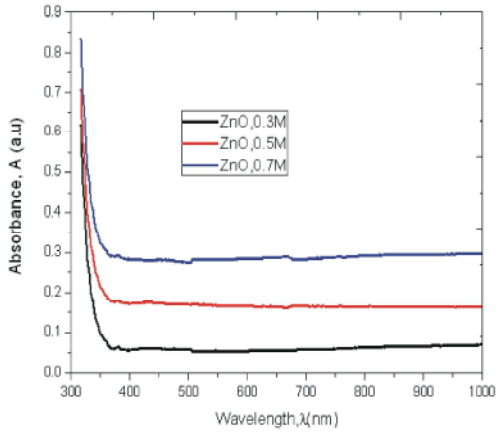

Fig. 1: Plot of A against λ for $Zn_{1-x}O$ films at different concentration

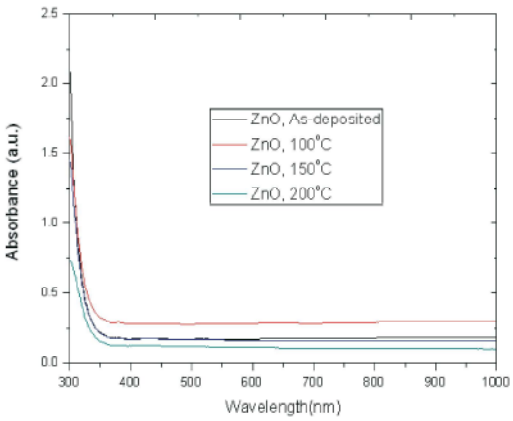

Fig. 2: Plot of A against λ for $Znn_{1-x}O$ films at different annealing temperature

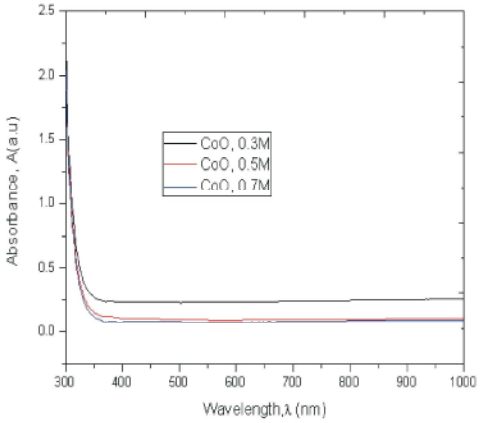

Fig. 3: Plot of A against λ for $Co_{1-x}O$ films at different concentration

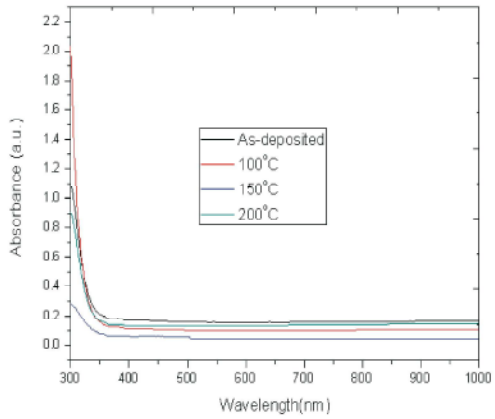

Fig. 4: Plot of A against λ for $Co_{1-x}O$ films at different annealing temperature

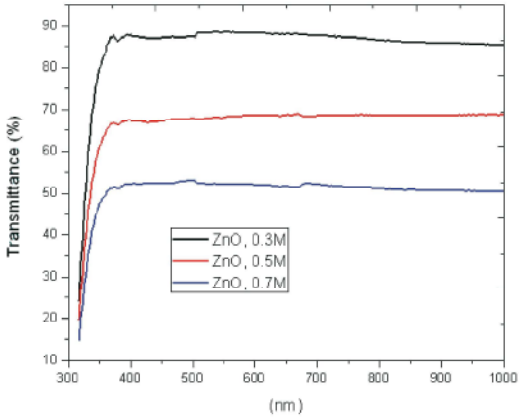

Fig. 5: Plot of T against λ for $Zn_{1-x}O$ films at different concentration

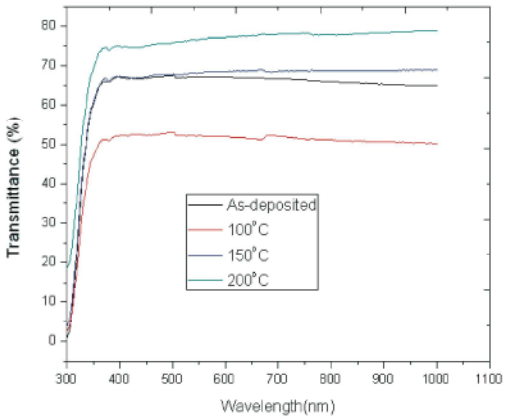

Fig. 6: Plot of T against λ for $Zn_{1-x}O$ films at different annealing temperature

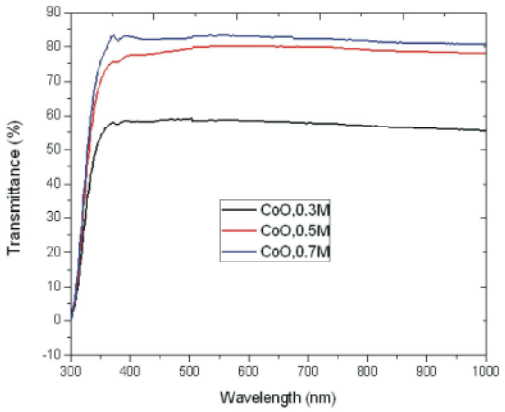

Fig. 7: Plot of T against λ for $Co_{1-x}O$ films at different concentration

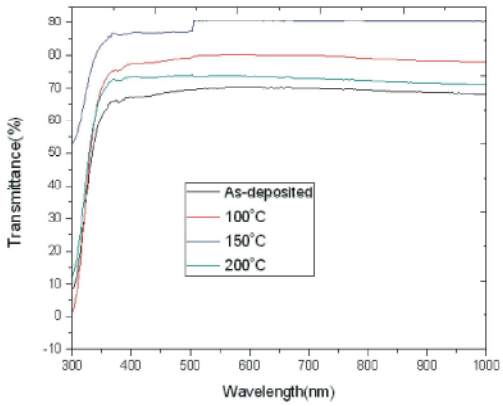

Fig. 8: Plot of T against λ for $Co_{1-x}O$ films at different annealing temperature

However, our report is at variance with that of Saleem *et al.* [30] for ZnO thin films deposited by sol-gel method. The transmittance decreasesd with concentration of precursor solution is based on the fact that at higher concentration, the constituent atoms will be more and more, leading to collision of incident light with atoms thus making it more difficult for light to pass through it [31-33]. It should be noted that when the concentration is high, the ions in solution would be high as well, leading to high rate of film formation. As such thicker films are grown at higher metallic precursor concentration. The relationship between the optical transmission and thickness is given by the Beer-Lambert equation as follows [34]:

$$T = \frac{I}{I_o} = e^{(-\alpha t)} \quad (1)$$

where **I** is the transmitted intensity at a particular wavelength, $\mathbf{I}_o$ is the incident light intensity, αis the absorption coefficient and t is the film thickness. The equation shows that the optical transmission of the ZnO films will decrease inversely proportional to the film thickness. The optical transmission is inversely proportional to the thickness of the films.The reduction of transmittance at higher molar concentration may also be attributed to the increased scattering of photons by increase of the roughness of the surface morphology [28]. With respect to post deposition temperature, the transmittance transparency varied from 2.5-67%, 2.5-53%, 5-68% and 22-80% for as-deposited, annealed at 100°C, 150°C and 200°C respectively. For$Co_{1-x}O$ films, it is noticed that the transmittance increased with precursor concentration from 2.5% to 60%, 2.5% to 80% and 2.5% to 85% for 03M, 0.5M and 0.7M respectively. Subjecting $Co_{1-x}O$ films to different temperatures, the transmittance varied from 10-68% for as-deposited, 2.5-77% for annealed at 100°C, 55-90% for annealed at 150°C and 10-74% for annealed at 200°C. The transmittance of thin films can be greatly modified by various growth parameters. In the literature, several authors have reported on the variation of transmittance with parametric investigation involving annealing temperature, concentration, dip time, P^H just to mention a few [35-43]. Fig. 9 shows the plots of absorption coefficient versus photon energy for $Zn_{1-x}O$ films at different concentration while Fig.10 shows the same plots at different annealing temperatures. Figures 11 and 12 show the plots of absorption coefficient versus photon energy for $Co_{1-x}O$ thin films for various concentrations and annealing temperatures respectively.

The absorption coefficient values of $Zn_{1-x}O$ films for parametric investigation involving concentration of precursor solution are generally much higher than of parametric variation of annealing temperature. The maximum α value is about $65x10^6m^{-1}$ for changes in concentration of precursor solution and $5x10^6m^{-1}$ for the latter. For $Co_{1-x}O$ films, the absorption coefficient spectra for both parameters of growth are similar exhibiting a maximum of about $5.5x10^6m^{-1}$ for variation of concentration and $4.75x10^6m^{-1}$ for changes in annealing temperatures. The high values of the optical absorption coefficients of $Zn_{1-x}O$ and $Co_{1-x}O$ films is an indication that the films may be suitable materials for various optoelectronic applications. For materials with a direct band gap, the correlation coefficient of absorption of the photon frequency satisfies the equation [44]:

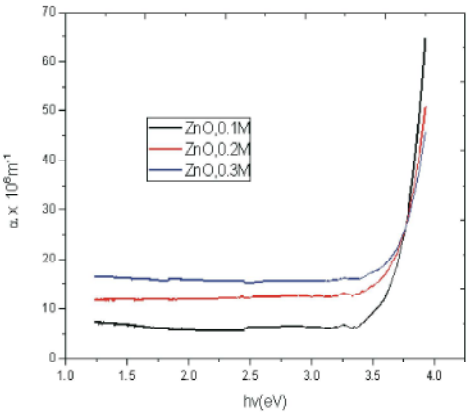

Fig. 9: Plot of α against hvfor $Zn_{1-x}O$ films various concentration

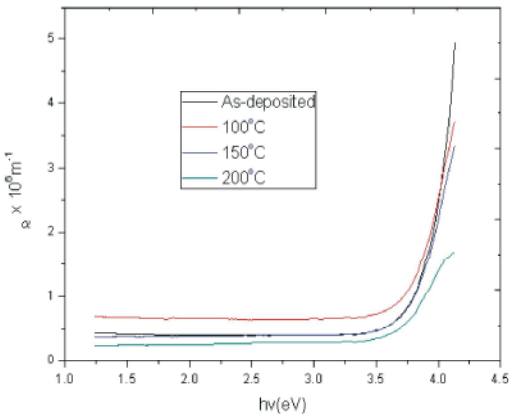

Fig. 10: Plot of α against hv for $Zn_{1-x}O$ films at different annealing temperature

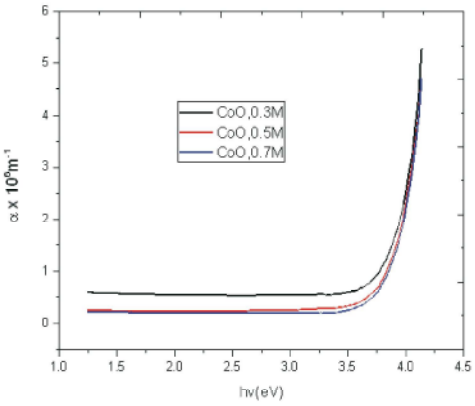

Fig. 11: Plot of α against hvfor $Co_{1-x}O$ films various concentration

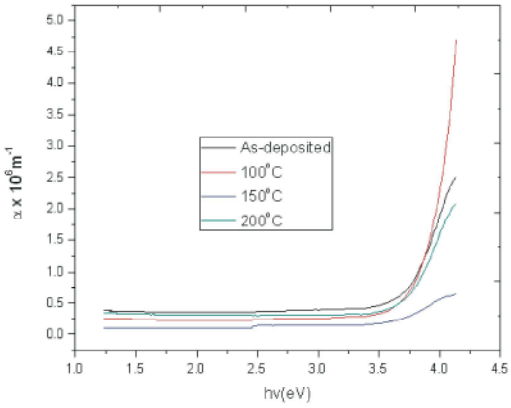

Fig. 12: Plot of α against hv for $Co_{1-x}O$ films at different annealing temperature

$$(\alpha hv)^2 = A(hv - E_g) \quad (2)$$

where α, h, v are absorption coefficient, planck's constant and photon frequency respectively. A is a constant and E_g is the band gap.Accordingly, the plots of $(\alpha hv)^2$ versus hv for $Zn_{1-x}O$ films at various concentration of precursor solution is shown in Fig. 13 while Fig. 14 shows the plots of $(\alpha hv)^2$ versus hv for $Zn_{1-x}O$ films at different annealing temperatures. Figures 15 and 16 are plots of $(\alpha hv)^2$ versus hv for $Co_{1-x}O$ films at different concentrations and annealing temperatures respectively.

With respect to Table 1, the band gap energy for $Zn_{1-x}O$ films lie from 3.68-3.75eV and 3.40-4.00eV for parametric variation of concentration and annealing temperature respectively. The band gap decreased with parametric investigation involving the two parameters of growth. The band gap narrowing induced by increase in the concentration of precursor solution may be due to the electron–electron and electron–impurity scattering. It is also possible that the energy absorbed more and more material which resulted to the wide band gap energy decreases.The band gap decreases with concentration observed in this work is collaborated with the reports of the following reference in the literature [27, 28, 33]. With respect to the band gap decreases with post deposition temperatures, we deduced that it could be attributed to the increase in grain size or related phenomena, caused by the annealing effects.This is collaborated by the fact that the band gap can be expressed in terms of the effective mass approximation [44].

$$\Delta E_g = \frac{\frac{\hbar^2\pi^2}{2R^2}\left(\frac{1}{M_e}+\frac{1}{M_h}\right)-\left(1.786e^2\right)}{\varepsilon R} \quad (3)$$

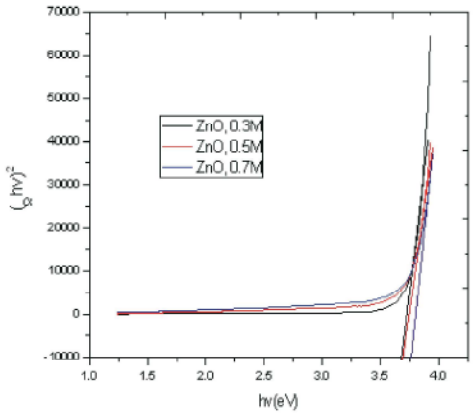

Fig. 13: Plot of $(\alpha hv)^2$ versus hvfor $Zn_{1-x}O$ films Ofilmsvarious concentration

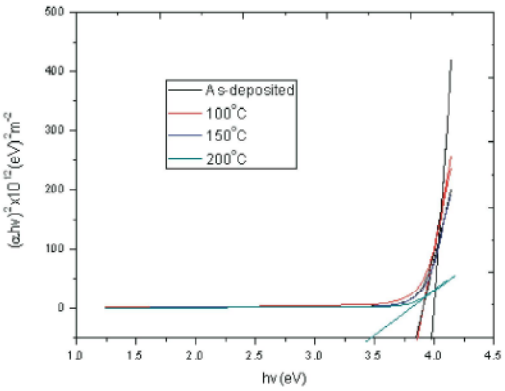

Fig. 14: Plot of $(\alpha hv)^2$ versus hv for Zn_{1-x} at different annealing temperature

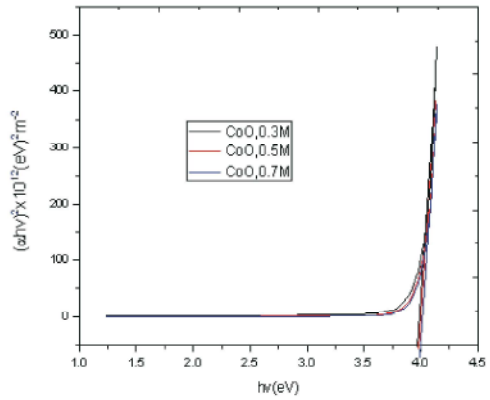

Fig. 15: Plot of $(\alpha hv)^2$ versus hvfor $Co_{1-x}O$ films for $Co_{1-x}O$ films various concentration

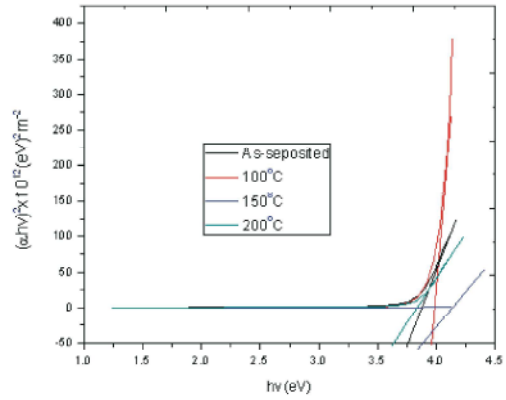

Fig. 16: Plot of $(\alpha hv)^2$ versus *hv* at different annealing temperature

Table 1: Band gap values of $Zn_{1-x}O$ films samples at different concentration and annealing temperature

Conc. (M)	E_g(eV)	Annealing temperature (°C)	E_g(eV)
0.3	3.75	As-deposited	4.00
0.5	3.70	100°C	3.85
0.7	3.68	150°C	3.84
		200°C	3.40

Table 2: Band gap values of $Co_{1-x}O$ films samples at different annealing temperature

Conc. (M)	E_g(eV)	Annealing temperature (°C)	E_g(eV)
0.3	4.00	As-deposited	3.75
0.5	4.01	100°C	3.90
0.7	4.05	150°C	3.85
		200°C	3.65

where M_e and M_h are the effective masses of the electrons in the conduction band and holes in the valance band respectively, ε is the static dielectric constant of the material and ΔE_g is the change in band gap of the semiconductor materials. The first term in the above equation represents the particle in-a-box quantum localization energy and has simple $1/R^2$ dependence, where R is the particle radius. The second term represents the Coloumb energy with 1/R dependence. Therefore, as R increases due to the increase in the crystallite size associated with high temperature annealing, the value of ΔE_g will decrease. Processes like annealing which increases the particle size decreases the band gap and occurs in most cases with post deposition annealing [45]. Also as temperature increases, the band gap decreases because the crystal lattice expands and the interatomic bonds are weakened. Our findings are in agreement with the report of other authors [46, 47]. With respect to Table 2, the band gap exhibited a blue shift with changes in molar concentrations and has on trend with post deposition temperature. At high concentrations, Fermi level shifts into the conduction band. Due to filling of the conduction band, absorption transitions occurs between valance band and Fermi level in the conduction band

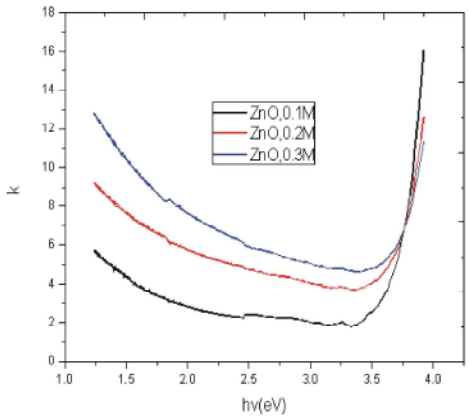

Fig. 17: Plot of k versus hvfor $Zn_{1-x}O$ films concentration

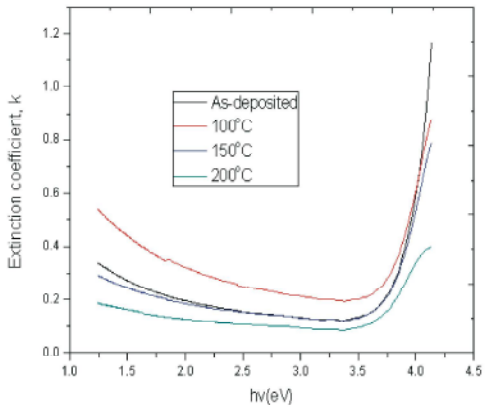

Fig. 18: Plot of k versus hv for $Zn_{1-x}O$ films various at different annealing temperature

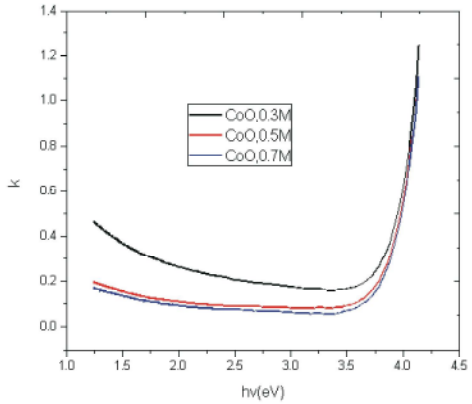

Fig. 19: Plot of k versus hvfor $Co_{1-x}O$ films concentration

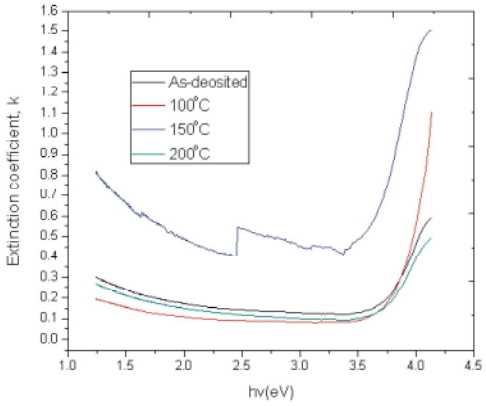

Fig. 20: Plot of k versus hv for $Co_{1-x}O$ films various at different annealing temperature

instead of valance band and bottom of the conduction band. This change in the absorption energy levels shifts the absorption edge to higher energies ε (blue shift) and leads to the energy band broadening.

The clear variation of E_g of the films with parameters of growth indicates that we can tune the solid state properties of films to suite a desired application. The high transparency in the visible region and wide direct band gap energy exhibited by these films make them ideal for use as window layer in a heterojunction solar cells. The use of wide band gap materials as window layers in solar cell fabrications is to minimize the recombination loss prevalent in direct band gap semiconductors thereby admitting a maximum amount of light to the junction region and the absorber layer. CdS thin films are widely used as window layer in CIGS solar cells. However, there are great concern about the toxicity of Cd in this architecture [48] and so; several alternative window layers are currently being investigated to replace CdS. In our view, $Zn_{1-x}O$ and $Co_{1-x}O$ films stand high for possible incorporation in CIGS solar cell. Fig. 17 shows the plot of extinction coefficient versus photon energy for $Zn_{1-x}O$ films at various concentration while Fig. 18 shows the plot of extinction coefficient versus photon energy for $Zn_{1-x}O$ films at different temperature. The plots of extinction coefficient versus photon energy for $Co_{1-x}O$ films are shown in Figures 19 and 20 for various concentrations and post deposition temperature respectively. A close look at Figures 17 and 18, indicates that the variations of extinction coefficient with photon energy have similar patterns fluctuating from a minima to maxima value. For $Zn_{1-x}O$ films, the extinction coefficient gradually increases with concentration decreases presumably due to increased surface optical scattering and optical loss, which induces the increase of extinction coefficient. The extinction coefficient also increases with annealing temperature decreases exhibiting a maximum for the as-deposited sample.

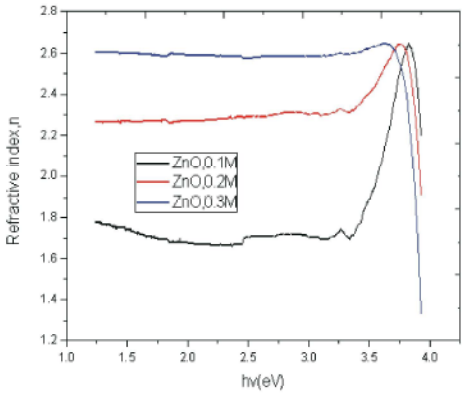

Fig. 21: Plot of n versus hvfor $Zn_{1-x}O$ films various concentration

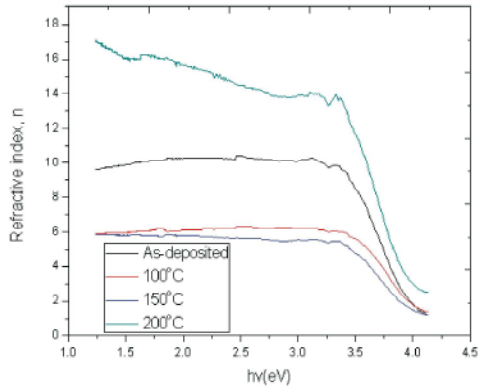

Fig. 22: Plot of n versus hv for $Zn_{1-x}O$ films at different annealing temperature

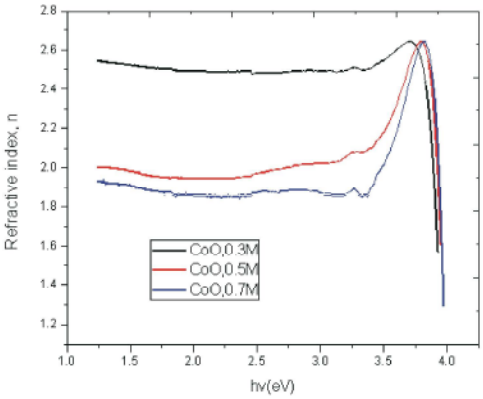

Fig. 23: Plot of n versus hvfor $Co_{1-x}O$ films various concentration

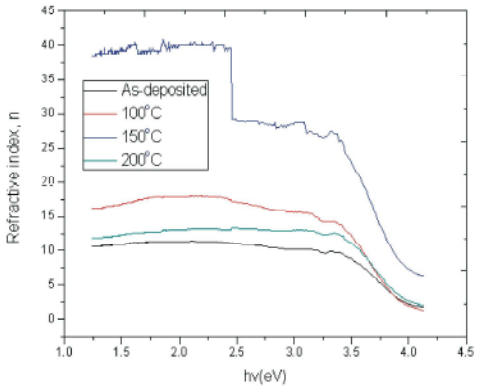

Fig. 24. Plot of n versus hv for $Co_{1-x}O$ films at different annealing temperature

The extinction coefficient of $Co_{1-x}O$ films vary in the same manner, increasing with concentration decreases exhibiting a maximum for 0.3M layer. With respect to post deposition temperature, no clear trend was observed. Figures 21 and 22 are plots of refractive index versus photon energy for $Zn_{1-x}O$ thin films at different annealing concentrations and post deposition temperature respectively. Figures 23 and 24 plots of refractive index versus photon energy for $Co_{1-x}O$ thin films at differentconcentration and post deposition temperature respectively.

The refractive index (n) of the thin films was calculated by the following relation [49].

$$n = \frac{1+R}{1-R} + \sqrt{\frac{4R}{\left(1+R^2\right)} - k^2} \quad (4)$$

where R is the normal reflectance and k is the extinction coefficient. As seen from Fig. 21, the refractive index increased with increase in the concentration of principal precursor solution within the photon energy range 1.25-3.5eV. The increase of refractive index with concentration may be explained on the basis of the contribution from both lattice distortion and the disorder of the films.With respect to post deposition temperature, the refractive index exhibited a downward trend. As observed in Fig. 23, the refractive index of $Co_{1-x}O$ films has the same maxima but different minima. Within 1.25-3.5eV, the refractive index of the 0.3M layer is generally higher compared to other layers. With respect to parametric investigation of annealing temperature, the refractive index shows a downward trend.

The plots of real parts of dielectric constant for parametric investigation involving changes in concentration and post deposition temperature for $Zn_{1-x}O$ thin films are shown in Figures 25 and 26 respectively while that of $Co_{1-x}O$ thin films are shown in Figures 27 and 28 respectively.

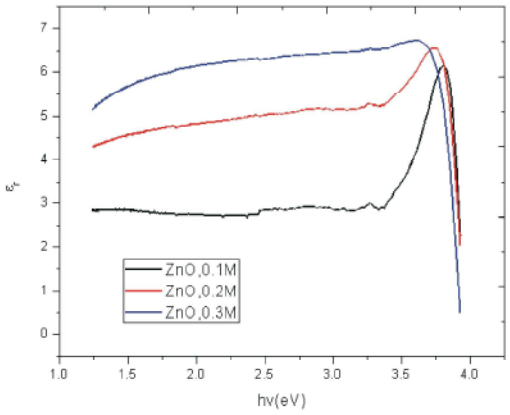

Fig. 25: Plot of ε_r versus hvfor $Zn_{1-x}O$ films various concentration

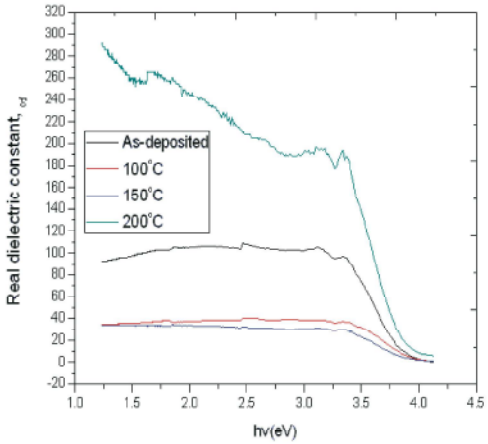

Fig. 26: Plot of ε_r versus hv for $Zn_{1-x}O$ films at different annealing temperature

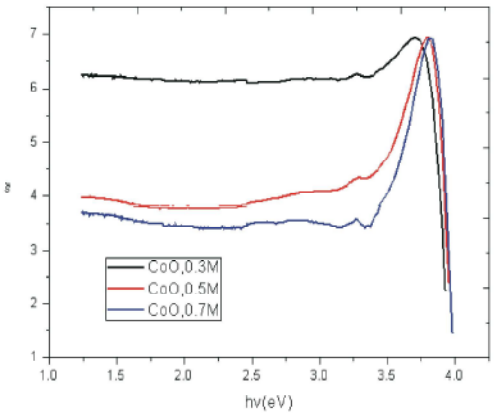

Fig. 27: Plot of ε_r versus hvfor $Co_{1-x}O$ films various concentration

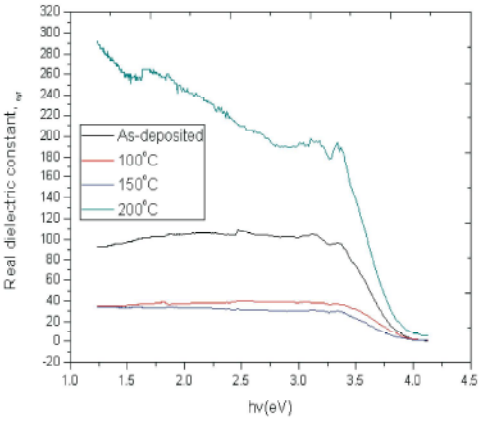

Fig. 28: Plot of ε_r versus hv for $Co_{1-x}O$ films at different annealing temperature

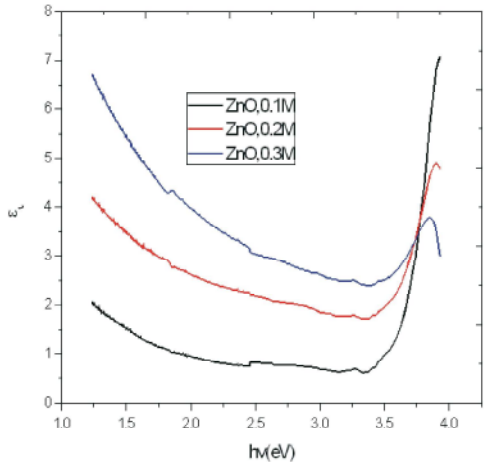

Fig. 29: Plot of ε_i versus hvfor $Zn_{1-x}O$ films various concentration

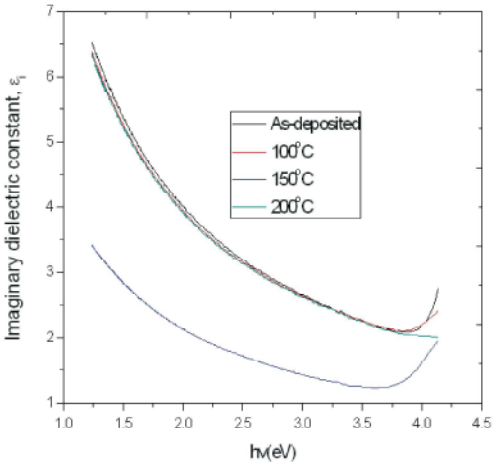

Fig. 30: Plot of ε_i versus hv for $Zn_{1-x}O$ films at different annealing temperature

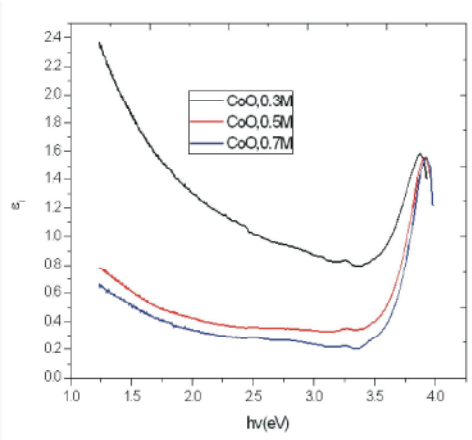

Fig. 31: Plot of ε_i versus hvfor $Co_{1-x}O$ films various concentration

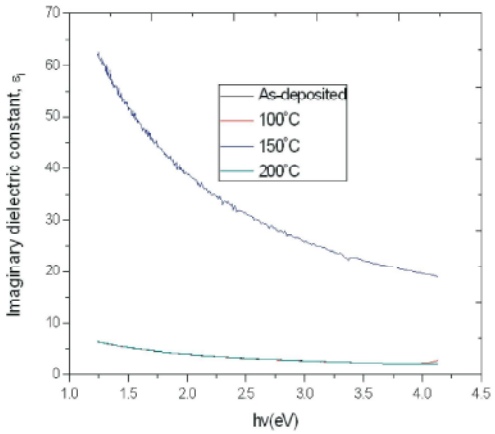

Fig. 32: Plot of ε_i versus hv for $Co_{1-x}O$ films at different annealing temperature

The complex dielectric constant is a fundamental intrinsic property of the material. The imaginary part shows how a dielectric material absorbs energy from an electric filed due to dipole motion. Fig. 29 shows the plot of imaginary dielectric constant versus photon energy for $Zn_{1-x}O$ thin films at different concentration while the plot of imaginary dielectric constant versus photon energy for $Zn_{1-x}O$ thin films at different annealing temperature is shown in Fig. 30. Figures 31 and 32 are plots of imaginary dielectric constant versus photon energy for $Co_{1-x}O$ thin films at different molar concentrations and annealing temperature respectively. From Fig. 29, ε_i decreased with photon energy up to 3.4eV and then increased. The imaginary dielectric constant generally lie in the range 0.5-7.3 for 0.3M layer, 1.5-5.0 for 0.5M layer and 2.5-6.8 for 0.7M layer. After thermal annealing, ε_i decreased up to 3.75eV and then increased exhibiting a minimum for annealed at 200°C. For $Co_{1-x}O$ films (Fig. 31), ε_i values are generally lower compared to that of $Zn_{1-x}O$ films. The imaginary dielectric constant generally vary from 0.8-2.4, 0.3-1.5 and 0.2-1.4 for 0.3M, 0.5M and 0.7M respectively. With respect to post deposition temperature, similar trend was observed.

CONCLUSIONS

In this study, we have grown $Zn_{1-x}O$ and $Co_{1-x}O$ thin films on glass substrate by chemical bath deposition method with 0.3 to 0.7 M zinc acetate and cobalt acetate concentrations. The deposited films were subjected to different annealing temperatures within the range 100-200°C. The optical and solid state properties of the films were investigated. It is found that all the optical parameters varied considerably with parameters of growth. It is found that the transmittance of $Zn_{1-x}O$ films decreased with concentration but increased with annealing temperature. $Zn_{1-x}O$ films transmittance transparency varies from 25-88%, 20-68% and 15%-53% at 0.3M, 0.5M and 0.7M respectively. For $Co_{1-x}O$ films, it is noticed that the transmittance increases with precursor concentration from 2.5% to 60%, 2.5% to 80% and 2.5% to 85% for 03M, 0.5M and 0.7M respectively. Subjecting $Co_{1-x}O$ films to different temperatures, the transmittance varies 10-68% for as-deposited, 2.5-77% for annealed at 100°C, 55-90% for annealed at 150°C and 10-74% for annealed at 200°C.For parametric investigation involving changes in concentration of $Zn_{1-x}O$ films, E_g lie from 3.68-3.75eV whereas for variation of annealing temperature, $E_g$attenuates from 3.40 to 4.00 eV. The band gap of $Co_{1-x}O$ films at different concentration increased from 4.00eV to 4.05eV whereas the band gap values at different annealing temperature lie between 3.65-3.90. In view of the various wide band gap energy exhibited by the films, they are promising window materials for solar cell fabrication as well as optoelectronic applications.

REFERENCES

1. Soki, T., Y. Hatanaka and D.C. Look, 2000. ZnO Diode Fabricated by Excimer-Laser Doping, Applied Physics Letters, 76(22): 3257-3259.
2. Lin. Y., C.R. Gorla, S. Linng, N. Emanetoglu, Y. Tor, H. Shen and M. Wraback, 2000. Ultraviolet Detectors Based on Epitaxial ZnO Films Grown by MOCVD, Journal of Electronic Materials, 29(1): 69-74.

3. Shinde, V.R., T.P. Gujar and C.D. Lokhande, 2007. LPG Sensing Properties of ZnO Films Prepared by Spray Py-rolysis Method: Effect of Molarity of Precursor Solu-tion," Sensors and Actuators H, 120(2): 551-559.
4. Ennaoui, A., S. Siebentrith, M. Ch. Lux-Steiner, W. Riedl and F. Karg, 2002. High-Efficiency Cd-Free CIGSS Thin-Film Solar Cells with Solution Grown Zinc Compound Buffer Layers, Solar Energy Materials and Solar Cells, 67(1-4): 31-40.
5. Chen, Y., D. Bagnall and T. Yao, 2000. ZnO as a Novel Pho- tonic Material for the UV Region, Materials Science and Engineering B, 75(2-3): 190-198.
6. Liang, S., H. Sheng, Y. Liu, Z. Hio, Y. Lu and H. Shen, 2000. Journal of Crystal Growth, 225: 110.
7. Koch, M.H., P.Y. Timbrell and R.N. Lamb, 1995. The Influence of Film Crystallinity on the Coupling Efficiency of ZnO Optical Modulator Waveguides, Semiconductor Science and Technology, 10(11): 1523.
8. Gulino, A.O., P. Dapporto, P. Rossi and I. Fragalà, 2003. No- vel Self-Generating Liquid MOCVD Precursor for Co3O4 Thin Films, Chemistry of Materials, 15(20): 3748-3752.
9. Lou, X.W., D. Deng. J.Y. Lee, J. Feng and L.A. Archer, 2008. Self-Supported Formation of Needlelike Co3O4 Nano-tubes and Their Application as Lithium-Ion Batteries Electrodes, Advanced Materials, 20(2): 258-262.
10. Lian, S., E. Wang, L. Gao and L. Xu, 2007. Fabrication of Sin-gle-Crystalline Co3O4 Nanorods via a Low-Temperature Solvothermal Process, Materials Letters, 61(18): 3893-3896.
11. Zou, D., C. Xu, H. Luo, L. Wang and T.I. Ying, 2008. "Synthe-sis of Co3O4 Nanoparticles via an Ionic Liquid-Assisted Methodology at Room Temperature, Materials Letters, 62(12-13): 1976-1978.
12. Poizot, P., S. Laruelle, S. Grugeon, L. Dupont and J. M. Tarascon, 2000. Nano-Sized Transition-Metal Oxides as Nega-tive-Electrode Materials for Lithium-Ion Batteries, Nature, 407(6803): 496-499.
13. Varghese, B., T.C. Hoong, Y.W. Zhu, M.V. Reddy, V.R. Chowdari, T.S. Wee, B.C. Vincent, C.T. Lim and C. Sow, 2007. Co3O4 Nanostructures with Different Morpholo-gies and Their Field-Emission Properties, General & In-troductory Materials Science, 17(12): 1932-1939.
14. Jiang, J. and L.C. Li, 2007. Synthesis of Sphere-Like Co_3O_4 Nan- ocrystals via a Simple Polyol Route, Materials Letters, 61(27): 4894-4896.
15. Li, Y., G.S. Tompa, S. Liang, C. Gorla and Y. Lu, 1997. Journal of Vacuum Science & Technology A, 15: 1063-1068.
16. Barreca, D., C. Massignan, S. Daolio, M. Fabrizio, C. Piccirillo, L. Armelao and E. Tondello, 2001. Composition and Microstructure of Cobalt Oxide Thin Films Obtained from a Novel Cobalt(II) Precursor by Chemical Vapor Deposition, Chemistry of Materials, *13* (2), 588-593 (2001). DOI: 10.1021/cm001041x
17. Ramakrishna K.T., H. Reddy, P.J. Gopalaswamy and R.W. Reddy, 2000. Miles, J. Crystal Growth, 210: 516-520.
18. Kadam, L.D., S.H. Pawar and P.S. Patil, 2001. Mat. Chem. Phy., 68: 280.
19. Jin-Hong, L. and P. Byung, 2003. Thin Solid Films, 426(1-2): 94-99.
20. Svegl, F., B. Orel, I.G. Svegl and V. Kaucic, 2000. Electr. Acta, 45: 4359.
21. Kon, M., P. Song, A. Mitsui and Y. Shigesato, 2002. Japan of Journal of Applied Physics, 41: 6174-6179.
22. Liao, C.L., Y.H. Lee, S.T. Chang, K.Z. Fuang and J. Pow, 2006. Sour., 158: 1379.
23. Lindroos, S. and M. Leskela, 2000. International Journal of Inorganic Materials, 2: 197-201.
24. Kandalkar, G., S. Gunjakar and J.L. Lokhande, 2008. Chandrakant. Preparation of cobalt oxide thin films and its use in supercapacitor application, Applied Surface Science - APPL SURF SCI. 254, 5540-5544.
25. Muhammad, M.A., 2011. Characterization of ZnO thin films grown by chemical bath deposition, Journal of Basrah Reseaarches (Sciences), pp: 37.
26. Chung-Wei, K., L. Chia-Yu, L. Ta-Jen, R. Vittal and H. Kuo-Chuan, 2011. Synthesis of cobalt oxide thin films by chemical bath deposition in the presence of different anions and applications to H_2O_2 sensing, Procedia Engineering, 25: 847-850.
27. Siregar, N., E. Marlianto and S. Gen, 2015. The effect of concentration of structure and optical properties of thin films synthesized by sol-gel methods spin coating, International Journal of Sciences: Basic and Applied Research, 22(1): 428-434.
28. Alami, Z.Y., M. Salem, M. Gaidi and J. Elkhamkham, 2015. Effect of Zn concentration on structural and optical properties of ZnO thin films deposited by spray pyrolysis, Advanced Energy: An international Journal, 2(4): 11-24.

29. Muzaffar, S.M., S. Khan, S. Riaz and S. Naseem, 2016. Effect on structural orientation of ZnO nanorods by changing the molarity and reaction time, Advances in Civil, Environmental and Materials Research (2016).
30. Saleem, M., L. Fang, H.B. Ruan, F. Wu, Q.L. Huang, C.L. Xu and C.Y. Kong, 2012. Effect of zinc acetate concentration on the structural and optical properties of ZnO thin films deposited by sol-gel method, International Journal of Physical Sciences, 7(23): 2971-2979.
31. Kamran, A.F.M., 2012. Effect of Sol Concentration on Structural and Optical Behavior of ZnO Thin Films Prepared by Sol-gel Spin Coating, International Journal of Applied Physics and Mathematics, 2(6).
32. Nagayasami, N. and S.G.V. Veerasamy, 2013. The Effect of ZnO Thin Films and Its Structural and Optical Properties Prepared By Sol-gel Spin Coating Method, Open Journal of Metal, Scientific Research.
33. Saleem, M., L. Fang, H.B. Ruan, F. Wu1, Q.L. Huang, C.L. Xu dan and C.Y. Kong, 2012. Effect of zinc acetate concentration on the structural and optical properties of ZnO thin films deposited by Sol-Gel method International Journal of Physical Sciences, 7(23): 2971-2979.
34. Reddy, V.S., K. Das, A. Dhar and S.K. Ray, 2006. The effect of substrate temperature on the properties of ITO thin films for OLED applications, Semiconductor Science and Technology, 21(12): 1747-1752.
35. Augustine, C., M.N. Nnabuchi, P.E. Agbo, F.N.C. Anyaegbunam, R.A. Chikenze, C.N. Nwosu, P.N. Kalu, U. Uba, R.O. Okoro and S.O. Onyishi, 2018. Investigation of the effect of lead ion (Pb^{2+}) concentration on the optical and solid state properties of chemically deposited $Mn_3O_4/Pb_{1-x}S$ heterojunction thin films, Journal of Ovonic Research, 14(5).
36. Augustine, C. and M.N. Nnabuchi, 2017. Band gap Determination of Novel PbS-NiO-CdO Heterojunction thin film for possible Solar Energy Applications, Journal of Ovonic Research, 13(4): 233-240.
37. Augustine, C., M.N. Nnabuchi, F.N.C. Anyaegbunam and A.N. Nwachukwu, 2017. Study of the effects of thermal annealing on some selected properties of Heterojunction PbS-NiO core-shell thin film, Digest Journal of Nanomaterials and Biostructures, 12(2): 523-531.
38. Augustine, C., M.N. Nnabuchi, F.N.C Anyaegbunam and C.U. Uwa, 2017. Annealing treatments and characterization of PbS-CdO core-shell thin film for solar energy applications, Chalcogenide Letters, 14(8): 321-329.
39. Augustine, C. and M.N. Nnabuchi, 2018. Optical and solid state characterization of chemically deposited CuO/PbS double layer thin film, Materials Research Express, 5(2): 1-11.
40. Augustine, C. and M.N. Nnabuchi, 2017. Band gap determination of chemically deposited lead sulphide based heterojunction thin films, Journal of Non-Oxide Glasses, 9(3): 85-98.
41. Augustine, C., and M.N. Nnabuchi, 2018. Mn_3O_4/PbS thin films: preparation and effect of annealing temperature on some selected properties, Materials Research Express, 5(3): 1-11.
42. Igweoko, A.E., C. Augustine, N.E. Idenyi, B.A. Okorie and F.N.C. Anyaegbunam, 2018. Influence of processing conditions on the optical properties of chemically deposited zinc sulphide (ZnS) thin film, 5: 1-12.
43. Chikwenze, R.A., 2012. Solution growth and characterization of binary selenide thin films for device applications, PhD. Thesis, Departmental of Industrial Physics, Ebonyi State University, Abakaliki, Ebonyi State, pp: 132-304.
44. Jing, Z., T. Xia, P. Yuan, F. Xiao and J. Zeng, 2010. Core/ Shell Structured Zn/SiO_2 Nanoparticles: Preparation Characterization and Photo catalytic property, Applied Surface Science, 257: 393-397.
45. Dipalae, J.D., S. Shaeed, S. Farha, G. Rrindam, B. Ravikiran, G. Anil and S. Ramphai, 2011. Effect of Annealing on the Structural and Optoelectronic properties of CdS Thin Film, Advance in Applied Science Research, 2(4): 471-425.
46. Ali, M.M., 2011. Characterization of ZnO thin films grown by chemical bath deposition, Journal of Basrah Researches (Sciences), 37(3A): 49-55.
47. Sanjeev, S. and D. Kekuda, 2015. Effect of annealing temperature on the structural and optical properties of zinc oxide (ZnO) thin films prepared by spin coating process, IOP Conferences Series: Materials Science and Engineering, 73: 012149.
48. Chopra, K.L., P.D. Paulson and V. Dutta, XXXX. Thin film solar cells: an overview, Prog Photovolt: Research Applications, 12: 69-92.
49. Cruz, J.S., D.S. Cruz, M.C. Arenas-Arrocena, F.D.M. Flores and S.A.M. Hernandez, 2015. Green synthesis of ZnS thin films by chemical bath deposition, Chalcogenide Letters, 12(5): 277-285.